

IL NUOVO CIMENTO  
DOI 10.1393/ncc/i2005-10173-6

VOL. 28 C, N. 4-5

Luglio-Ottobre 2005

## Characteristics and performance of the Swift X-Ray telescope<sup>(\*)</sup>

G. TAGLIAFERRI<sup>(1)</sup>, S. CAMPANA<sup>(1)</sup>, G. CHINCARINI<sup>(1)(2)</sup>, O. CITTERIO<sup>(1)</sup>  
A. MORETTI<sup>(1)</sup>, P. ROMANO<sup>(1)</sup>, D. N. BURROWS<sup>(2)</sup>, J. E. HILL<sup>(2)</sup>, J. KENNEA<sup>(2)</sup>  
D. C. MORRIS<sup>(2)</sup>, J. A. NOUSEK<sup>(2)</sup>, C. PAGANI<sup>(1)(3)</sup>, A. WELLS<sup>(4)</sup>, A. F. ABBEY<sup>(4)</sup>  
A. BEARDMORE<sup>(4)</sup>, M. R. GOAD<sup>(4)</sup>, J. OSBORNE<sup>(4)</sup>, K. PAGE<sup>(4)</sup>, M. CAPALBI<sup>(5)</sup>  
P. GIOMMI<sup>(5)</sup>, M. PERRI<sup>(5)</sup>, F. TAMBURELLI<sup>(5)</sup>, L. ANGELINI<sup>(6)</sup>, G. CUSUMANO<sup>(7)</sup>  
V. MANGANO<sup>(7)</sup>, V. LA PAROLA<sup>(7)</sup>, and G. D. HARTNER<sup>(8)</sup>

<sup>(1)</sup> *INAF-Osservatorio Astronomico di Brera - via Bianchi 46, 23807 Merate, Italy*

<sup>(2)</sup> *Università di Milano-Bicocca - piazza della Scienza 3, 20126 Milano, Italy*

<sup>(3)</sup> *Penn State University - 525 Davey Lab, University Park, PA 16802, USA*

<sup>(4)</sup> *University of Leicester - University Road, Leicester LE1 7RH, UK*

<sup>(5)</sup> *ASI-ASDC - Via Galileo Galilei, 00044 Frascati, Italy*

<sup>(6)</sup> *NASA-GSFC - Greenbelt, MD 20771, USA*

<sup>(7)</sup> *INAF-IASF Palermo - Via Ugo La Malfa 153, 90146, Palermo, Italy*

<sup>(8)</sup> *Max-Planck-Institut für Extraterrestrische Physik - Garching, Germany*

(ricevuto il 23 Maggio 2005; pubblicato online il 2 Novembre 2005)

**Summary.** — The X-ray Telescope (XRT), on board the Swift satellite, has been built to provide: automated source detection and position with few arcsecond accuracy within 5 seconds of target acquisition; CCD spectroscopy and imaging capability (0.2–10 keV), with a detection sensitivity of  $2 \times 10^{-14}$  erg cm<sup>-2</sup> s<sup>-1</sup> in 10<sup>4</sup> s; automatic adjusting of the CCD readout mode to optimize the science return as the source fades. XRT can observe GRB afterglows over several orders of magnitude in flux. The first results obtained during the in-flight performance verification phase confirm that XRT is fully compliant with the requirements and is providing excellent results.

PACS 95.55.Ka – X- and  $\gamma$ -ray telescopes and instrumentation.

PACS 95.85.Nv – X-ray.

PACS 98.70.Rz –  $\gamma$ -ray sources;  $\gamma$ -ray bursts.

PACS 01.30.Cc – Conference proceedings.

<sup>(\*)</sup> Paper presented at the “4th Workshop on Gamma-Ray Burst in the Afterglow Era”, Rome, October 18-22, 2004.

## 1. – Introduction

After the discoveries made by the *BeppoSAX* satellite it was clear that if we wanted to properly study Gamma-Ray Bursts (GRB) and in particular the associated afterglows, we needed a fast-reaction satellite capable of detecting GRBs and of performing immediate multiwavelength follow-up observations. Swift [6] is designed specifically to study GRBs and their afterglow in multiple wavebands. It was successfully launched on 2004 November 20, opening a new era in the study of GRBs. Swift has on board three instruments: a Burst Alert Telescope (BAT) that detects GRBs and determines their positions in the sky with an accuracy better than 4 arcmin in the band 15–350 keV [1]; an UV-Optical Telescope (UVOT) capable of multifilter photometry with a sensitivity down to 24<sup>th</sup> magnitude in white light and a 0.3 arcsec positional accuracy [7]; an X-ray Telescope (XRT) providing fast X-ray photometry and CCD spectroscopy in the 0.2–10 keV band with a positional accuracy better than 5 arcsec. Here we will briefly describe the XRT overall properties and provide its earliest in-flight performance. For a more detailed description of the XRT characteristics see [2,3].

## 2. – Overall description and performance

The XRT imaging capabilities are provided by a grazing incidence Wolter I telescope that focuses the X-rays onto a CCD at a focal length of 3.5 meters. The mirror module is made of 12 nested gold-coated electroformed Ni mirrors. Two thermal baffles in front of the mirror maintain the mirror temperature at a constant value of about 20° C and prevent temperature gradients that would degrade the image quality. The focal plane camera houses the CCD, four calibration sources that illuminate the CCD corners continuously, an optical blocking filter and a thermo-electric cooling (TEC) system capable of maintaining the CCD temperature at –100° C, with the heat dumped to a radiator sitting at a temperature between –85° C and –45° C, depending on orbital parameters and spacecraft orientation. The CCD is a 600 × 600 array of 40 μm × 40 μm pixels, each corresponding to 2.36 arcseconds. A telescope alignment monitor (TAM) provides an accurate measurement of the alignment between the XRT boresight and the star trackers that are directly mounted on the XRT forward tube. The XRT structure is provided by an optical bench interface flange (OBIF) on which the forward telescope tube is mounted, supporting the star trackers and the telescope door, and the rear tube supporting the focal plane camera. The mirror module, which is inside the front tube, is mounted directly on the OBIF through a mirror collar. Electron deflection magnets are placed behind the rear face of the OBIF to prevent electrons that pass through the mirror from reaching the detector. The OBIF provides also the mounting interface to the structure of the Swift satellite.

The main XRT science requirements were: rapid, accurate positions (better than 5 arcsec in less than 100 seconds after the burst), moderate resolution spectroscopy (better than 400 eV at 6 keV after three years of operation) and accurate photometry for sources spanning up to seven order of magnitude in flux with a time resolution better than 10 ms. To achieve the latter goal two timing modes have been implemented: the Photodiode mode that provides a time resolution of 0.14 ms, but integrates the count rate over the entire CCD (so it has no image capability), and the Windowed Timing mode that provides 2 ms time resolution with spatial resolution along one direction (1-D image). Two other modes complete the observing capabilities of XRT: the Image mode, that provides only image information but no spectroscopic data, and the Photon-counting mode that provides the full imaging and spectroscopic information with a time resolution

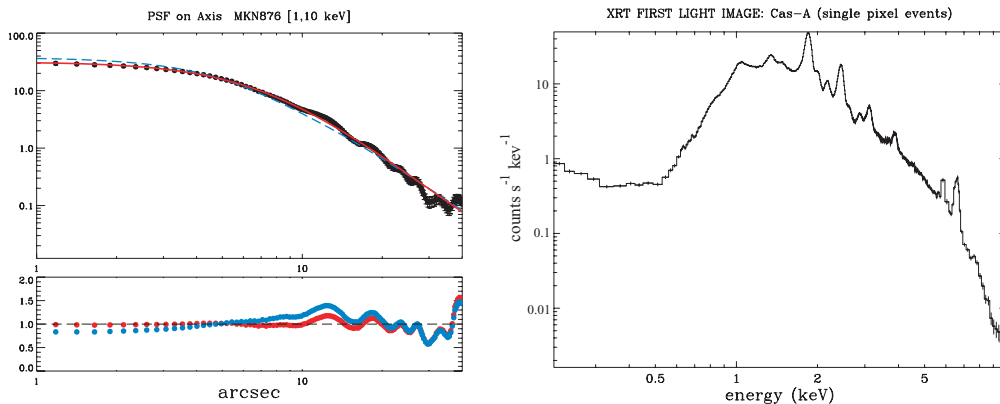


Fig. 1. – The left panel shows the XRT PSF as measured in-flight on the bright source MKN 876. Note how the in flight PSF (continuous line) agrees perfectly with the one measured on ground (dashed line). The right panel shows the X-ray spectrum of Cas-A, with various emission lines detected. The XRT spectral resolution of  $\sim 140$  eV agrees with the one measured on ground.

of 2.5 seconds. This is the standard mode in which XRT will be operated for sources with fluxes below 1 mCrab. In order to be able to properly observe sources that are rapidly changing in flux, as is the case with GRBs and their afterglows, the XRT will automatically change the readout mode based on the source intensity.

To establish the XRT performance an end-to-end calibration campaign was performed in September 2002 at the Panter X-ray calibration facility in Munich. This allowed us to verify that the XRT Point Spread Function has a HEW of 18 arcsec at 1.5 keV (22 arcsec at 8.1 keV) and it is quite uniform over the entire field of view. The total effective area of XRT is of  $\sim 135$  cm<sup>2</sup> at 1.5 keV. The Panter tests also demonstrated that XRT is capable of determining the source position with the required accuracy and of autonomously and correctly changing its readout mode accordingly with the varying source flux.

After the Swift launch, the XRT was turned on 2004 November 23, but remained with the door closed while outgassing of the various components took place. After about two weeks the telescope door was successfully opened. However, during the complete activation phase of XRT a major problem arose: the TEC system stopped functioning, leaving the temperature control of the CCD detector only under the passive radiator system. Thus, in order to prevent that the CCD gets too hot and it loses sensitivity at low energies, more stringent pointing constraints have been implemented to keep the CCD temperature below  $-50^\circ$  C (this guarantees that XRT performs as expected). Since then Swift has been successfully operated maintaining the CCD temperature below this value. The first light occurred on December 11, when Swift was pointed to the bright supernova remnant Cas-A. XRT provided a superb image that shows structures and filaments at different temperatures. After the first light observation the calibration campaign started and various known X-ray targets were observed to verify: the PSF as a function of the off-axis angle; effective area; timing capability; spectral energy resolution and capability of determining the source location. All measurements that were made during the end-to-end test at the Panter facility have been verified, confirming the perfect functioning of XRT (see, *e.g.*, fig. 1).

Of course while Swift was performing its calibration campaign it was already able to

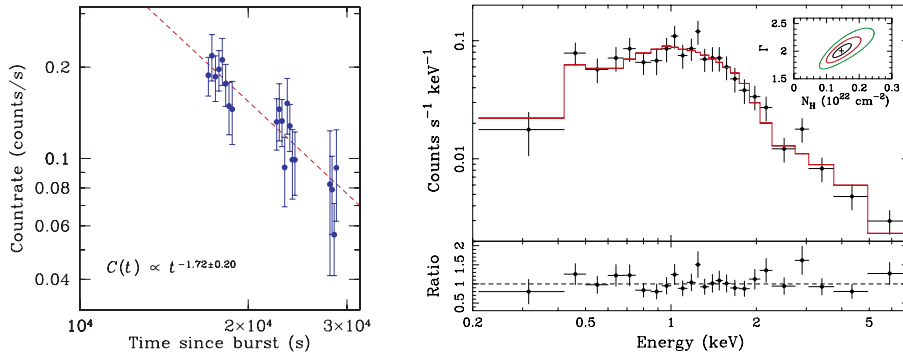


Fig. 2. – The left panel shows the X-ray light curve of GRB041223, while the right panel shows its X-ray spectrum with the best-fit absorbed power law model. The inset shows 1, 2 and  $3\sigma$  confidence contours for the photon index and  $N_H$ .

detect GRBs. Indeed various GRBs have been detected by BAT and up to the end of February nine were also observed with the XRT. Of these nine, four were repointed in less than 200 seconds, while the other five were repointed with a delay of few hours due to pointing constraints. In all nine cases an X-ray source associated with the GRB has been detected and their coordinates have been immediately distributed via the GCN network system. Follow-up on ground observations have identified the optical/NIR counterpart for four of them. The comparison of the afterglow XRT coordinates and those from the on-ground observations shows that the average positional accuracy of XRT in locating the GRB position is 2.1 arcsec: a factor 2.5 better than the requirements. The first GRB observed by XRT occurred on 2004 December 23 [4]. In fig. 2 we show the X-ray light curve and spectrum of the afterglow associated to GRB041223 as measured by the XRT (see also [5] for a report on GRB050128 promptly observed by XRT). In conclusion the XRT in-flight performance verification phase and the observations of the first few GRBs confirm that XRT is fully functional and it is providing excellent results.

## REFERENCES

- [1] BARTHELMY S. D. *et al.*, *SPIE*, **5165** (2004) 175.
- [2] BURROWS D. N. *et al.*, *SPIE*, **5165** (2004) 201.
- [3] BURROWS D. N. *et al.*, *Space Sci. Rev.*, (2005) in press.
- [4] BURROWS D. N. *et al.*, *ApJ*, **622** (2005) L1.
- [5] CAMPANA S. *et al.*, *ApJ*, **625** (2005) L23; astro-ph/0504331.
- [6] GEHRELS N. *et al.*, *ApJ*, **611** (2004) 1005.
- [7] ROMING P. N. *et al.*, *SPIE*, **5165** (2004) 217.